Population Density Measurements in a Partially Ionized Freejet Expansion Flow

Akira Kimura and Michio Nishida

Department of Aeronautical Engineering, Kyoto University, Kyoto, Japan

(Z. Naturforsch. **32 a**, 84–87 [1977]; received October 22, 1976)

Population densities of the 4p and 5p levels of argon atoms were measured along a freejet centerline of partially ionized argon in a low density plasma wind tunnel. The measured axial distribution of the 4p[3/2] level population has been compared with a theoretical prediction using a modified Thomson's formula for the excitation cross sections.

The study of nonequilibrium populations in rapidly expanding plasma flows is interesting because of possible population inversions leading to lasers by fluidmechanical means. Such measurements have been carried out by a few workers [1–3]. In the present work the population densities of argon atoms in a partially ionized freejet have been measured. The measured axial distributions of population densities have been compared with predicted ones. The excited levels of the argon atoms have been subdivided into four quasistates (cf. Table 1). This model is similar to that used by Hollenbach and Salpeter [4], and also somewhat similar to that used by Wojciechowski and Weymann [5].

Table 1.

Level no. j	Term value E_j (eV)	Statistical weight g_j	Electron configuration
0	0	1	$(3p^6)$
1	11.7	12	$(3p^5)\,4s$
2	13.1	36	$(3p^5)\,4p$
3	14.1	72	$(3p^5)\,3d$, 5s
4	14.85	288	$(3p^5)\,4d$, 5p, 6s, 4f, 6p, 5d

Since the flow properties along the freejet centerline are very similar to a source flow expansion [6], the continuity equation for the population of the jth level may be written as

$$\frac{1}{r^2}\frac{\mathrm{d}}{\mathrm{d}r}\left[r^2 N(j) u\right] = \dot{N}(j)\,, \tag{1}$$

where r is the distance from a source, u the velocity, $N(j)$ the population density of the jth level and $\dot{N}(j)$ the net production rate of the population of the jth level. Introducing $\alpha_j = N(j)/N$, where N is the overall density, and noticing that $r^2 N u =$ const, we can rewrite Eq. (1) in the form

$$\mathrm{d}\alpha_j/\mathrm{d}r = r^2 \dot{N}(j)/r_0^2 N_0 u_0\,, \tag{2}$$

where the subscript 0 denotes the reference point. According to Ashkenas and Sherman [6], the freejet streamlines appear to radiate from a source at a distance x_0 downstream of the orifice and a value of x_0/D, where D is the orifice diameter, is 0.075 for a monatomic gas. Hence the distance from the source, r, may be taken as the distance from the orifice, x, if the measurements are made sufficiently far from the orifice.

The following assumptions can be introduced under the present experimental conditions: (1) Net population rates incoming from and outgoing to adjacent levels are only considered, (2) ionizations and recombinations are neglected as compared with excitations and de-excitations. Under these assumptions the net population rate of the jth level, $\dot{N}(j)$, is expressed by

$$\begin{aligned}\dot{N}(j) = {} & N_e[N(j+1)Q(j+1,j) \\ & + N(j-1)Q(j-1,j)] \\ & - N_e N(j)[Q(j,j+1) + Q(j,j-1)] \\ & + \sum_{s=j+1}^{4} A(s,j) N(s) - \sum_{s=0}^{j-1} A(j,s) N(j)\,,\end{aligned} \tag{3}$$

where $Q(s,j)$ is the collisional rate constant for a transition from the sth level to the jth level through the impact by an electron and $A(s,j)$ the Einstein A coefficient for a radiative transition from the sth level to the jth level $(s>j)$. The collisional excitation rate constant estimated from the modified Thomson's formula for an excitation cross section [7] is adopted here. The collisional de-excitation rate constant is easily determined by means of the principle of detailed balance. The radiative transition probabilities given in Ref. [8] are used in the present work.

Experiments have been carried out in a low density plasma wind tunnel operated by a d.c. arc discharge with a maximum power of 25 kW. The performance of this facility is described in detail in Ref. [9]. The test section, a cylinder with 90 cm diameter and 110 cm length, is connected with a 2600 liters vacuum tank. The test gas, which is heated and partially ionized by an arc heater, flows into a plenum chamber which is 78 mm wide and 216 mm long, and then expands through an orifice with a diameter of 13.7 mm into the test section as a freejet. In order to make spectroscopic measurements along the freejet centerline in the fixed optical system, the position of the orifice is movable. Typical operating conditions are as follows: mass flow is 0.112 g/sec; stagnation pressure 12.6 Torr; test section pressure 0.095 Torr; stagnation temperature 3200 K.

The impact pressure along the freejet centerline has been measured by means of a conventional impact pressure probe. It was found that the impact pressure is proportional to $(x/D)^{-2}$ from $x/D=1.1$ to the Mach disk position, showing that the present freejet can be replaced by a source flow expansion. It was also shown from an isentropic relation that the Mach number and atom density vary from 2.9 and $4.1\times10^{15}\,\mathrm{cm}^{-3}$ at $x/D=1.1$ to 8.5 and $1.9\times10^{14}\,\mathrm{cm}^{-3}$ at $x/D=5$.

The electron temperatures and densities have been measured by means of a conventional plane Langmuir probe which was made of a 0.5 mm diameter tungsten wire coated with an alumina ceramic. The electron temperature decreases from 3800 K at $x/D=1.1$ to 1500 K at $x/D=3$, and then increases in front of a Mach disc. This increase is due to the large thermal conductivity of electrons [10, 11]. The electron density varies from $1.6\times10^{13}\,\mathrm{cm}^{-3}$ at $x/D=1.1$ to $1.7\times10^{12}\,\mathrm{cm}^{-3}$ at $x/D=5$. These electron temperatures and densities have been employed to solve Equation (2).

The spectroscopic system is also shown in Figure 1. The intermediate-image method was used for the slit lighting, and the focal distances of the quartz lenses F_1 and F_2 were 32.20 cm and 16.50 cm, respectively. An intermediate slit L was placed immediately behind the lens F_2 in order to reduce the light from outside the neighborhood of the centerline of the freejet. A Shimadzu GE 100 Ebert type plane diffraction grating spectrograph has been used (range of wavelengths 2000 Å – 11000 Å, focal distance of the main concave mirror 100 cm, grating number of 600/mm, grating area of $52\times52\,\mathrm{mm}^2$,

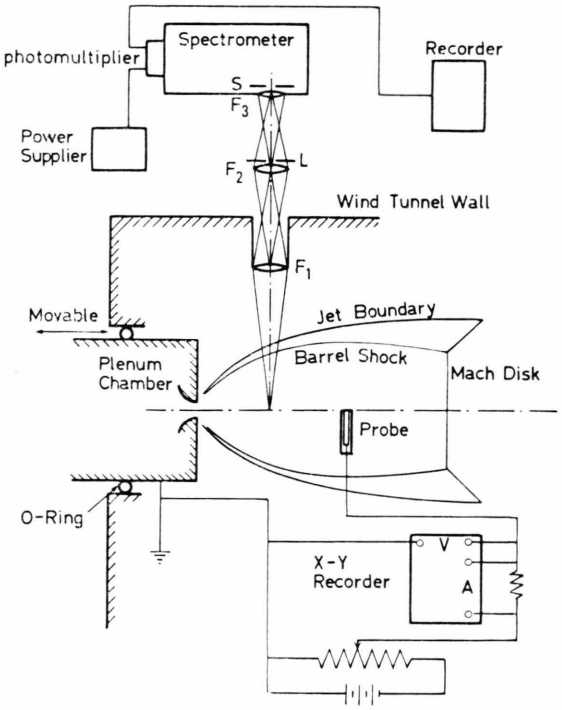

Fig. 1. Schematic digram of measurements.

first order inverse dispersion 16.6 Å/mm). The spectra were taken by a photomultiplier system.

We have measured intensities of spectral lines corresponding to the transitions 4s – 5p (from the fourth to the first quasistate) and 4s – 4p (from the second to the first quasistate). The lines were AI 4044, 4159, 4522 for the 4s – 5p transition and AI 7635 for the 4s – 4p transition.

The axial distributions of the measured population densities of the levels 5p′[3/2], 5p[3/2], and 5p[1/2] are shown in Figure 2. From these the population density of the fourth quasistate as a function of x/D was evaluated.

Figure 3 shows the axial distribution of the population density of the 4p[3/2] level, which has been evaluated from the intensity of the line AI 7635. Also shown are predicted curves for the level 4p[3/2]. $R=0$ and $R\neq0$ denote the optically thick and thin cases for the 0 – 1 transition, respectively. In both cases the populations of the first, second and third quasistates at the starting point of the calculation have been determined from the steady state condition, while the population of the fourth quasistate has been estimated from the measurements. With these initial populations Eq. (2) has

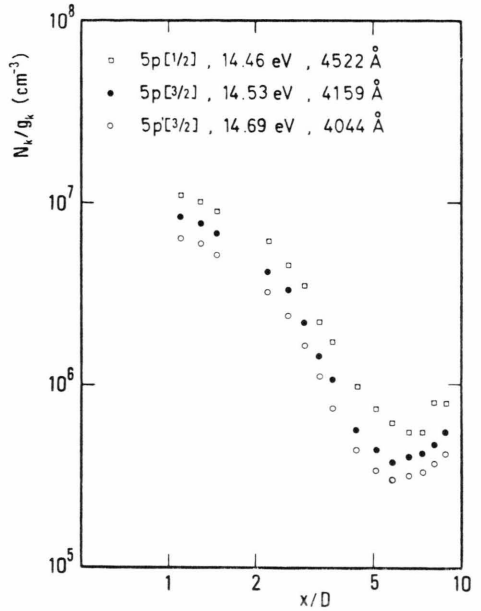

Fig. 2. Population density distributions of the 5p levels.

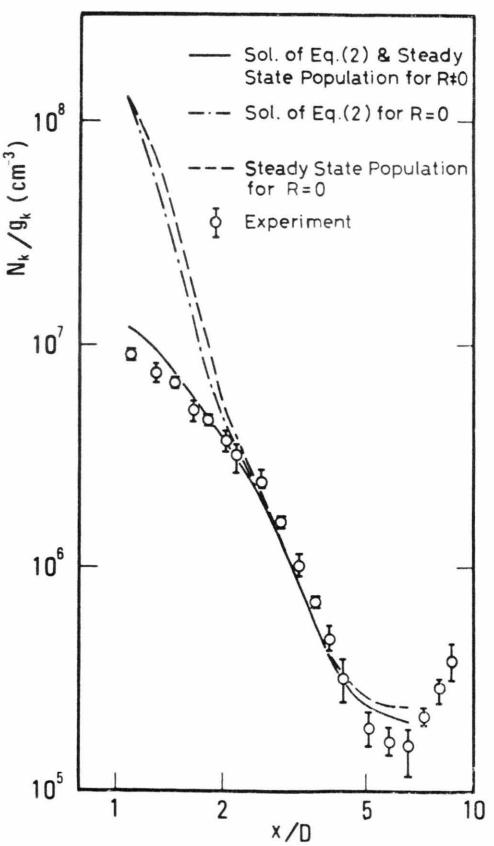

Fig. 3. Comparison between measured population density distribution of the 4p[3/2] level and predicted one.

been numerically solved for each quasistate. The populations were estimated from the calculated results of α_j, with the use of N estimated from the isentropic relation. In Fig. 3 the predicted curve in the optically thin case for the $0-1$ transition is in fairly good agreement with the experimental result. The initial value of the 4p[3/2] level population in the optically thick case for the $0-1$ transition is larger than the experimental result by an order of magnitude. However, in the downstream of $x/D \cong 2.5$ the calculated results for both cases coincide. On the other hand, instead of solving Eq. (2) the population densities have been calculated under the assumption of steady state population. As shown in Fig. 3, they are in good agreement with those obtained from the solution of Equation (2). It is therefore more convenient to discuss the difference between the optically thin and thick cases for the $0-1$ transition by means of the results of the steady state populations. Under the steady state condition the population density of the second quasistate is expressed in terms of $N(4)$ as

$$N(2) = \frac{a_{23}\,a_{34}}{a_{22}\,a_{33}} \frac{1+K_3+K_4}{1-K_1-K_2} N(4) \qquad (4)$$

$$\cong \frac{a_{23}\,a_{34}}{a_{22}\,a_{33}} \frac{1+K_3}{1-K_2} N(4)$$

where $K_1 = a_{23}\,a_{32}/a_{22}\,a_{33}$, $K_2 = a_{12}\,a_{21}/a_{11}\,a_{22}$, $K_3 = a_{24}\,a_{33}/a_{23}\,a_{34}$, $K_4 = a_{14}\,a_{21}\,a_{33}/a_{11}\,a_{23}\,a_{34}$. a_{jj} denotes the total transition probability from the jth quasistate and a_{jk} the transition probability from the kth quasistate to the jth one. Since K_1 and K_4 are very small compared with unity, these terms have been neglected. In Eq. (4) the term including $N(0)$ is also neglected since it is extremely small compared with unity. The factor $(a_{23}\,a_{34}/a_{22}\,a_{33})\,(1+K_3)$ is common in both the optically thick and thin cases for the $0-1$ transition, and the remaining factor $1/(1-K_2)$ expresses the difference between both cases. For the optically thick case for the $0-1$ transition, the factor $K_2 = a_{12}\,a_{21}/a_{11}\,a_{22}$ varies from 0.88 at $x/D = 1.1$ (the starting point) to 0.016 at $x/D = 3.0$ and then slightly increases up to 0.052 at $x/D = 5.0$ while for the optically thin case for the $0-1$ transition it varies from 7.8×10^{-4} at $x/D = 1.1$ to 1.9×10^{-7} at $x/D = 3$ and also slightly increases up to 3.1×10^{-7} at $x/D = 5$. The slight increase in this factor at $x/D = 3$ corresponds to the increase in the electron temperature in front of the Mach disc. For the optically thick case for the $0-1$

transition one may mention that in the downstream of $x/D \cong 3$ the contribution of the factor K_2 to the estimation of $N(2)$ is close to that in the optically thin case for the $0-1$ transition. The ratio a_{12}/a_{22} is of the order of unity in the entire region of the freejet. Hence the ratio a_{21}/a_{11} controls the factor $K_2 = a_{12}\, a_{21}/a_{11}\, a_{22}$. In the optically thick case for the $0-1$ transition the values of a_{11} and a_{21} vary from $2.6 \times 10^5\ \mathrm{sec}^{-1}$ and $2.4 \times 10^5\ \mathrm{sec}^{-1}$ at $x/D = 1.1$ to $1.8 \times 10^3\ \mathrm{sec}^{-1}$ and $9.3 \times 10^1\ \mathrm{sec}^{-1}$ at $x/D = 5$, respectively. Hence one may state that far downstream the population of the second quasistate in the optically thick case for the $0-1$ transition is similar to that in the optically thin case. This situation in the downstream of $x/D = 3$ results in the predicted curve as shown in Figure 3.

In the present experiment only the populations of 4p[3/2], 5p[1/2], 5p[3/2] and 5p′[3/2] were measured and as a preliminary study the axial distribution of the measured 4p[3/2] level population has been discussed in comparison with the predicted one, which shows that the measured populations are in agreement with those predicted from the steady state condition, in the optically thin case for the $0-1$ transition. In order to insure further this result population measurements of the first quasistate should be done.

[1] P. Hoffmann and W. L. Bohn, Z. Naturforsch. **22 a**, 1953 [1967].
[2] C. Park, J. Plasma Phys. **9**, 217 [1973].
[3] D. D. McGregor and M. Mitchner, Phys. Fluids. **17**, 2155 [1974].
[4] D. J. Hollenbach and E. E. Salpeter, J. Chem. Phys. **50**, 1157 [1969].
[5] P. H. Wojciechowski and H. D. Weymann, J. Chem. Phys. **61**, 1369 [1974].
[6] H. Ashkenas and F. S. Sherman, Rarefied Gas Dynamics, Vol. II, Toronto, Canada, 84 (1965).
[7] Y. M. Kogan, R. I. Lyaguschenko, and A. D. Khakhaev, Opt. Spectrosc. **15**, 5 [1963].
[8] W. L. Wiese, M. W. Smith, and B. M. Miles, NSRDS-NBS **22** [1969].
[9] M. Nishida, Doctoral Thesis, Kyoto University, Kyoto, Japan 1969.
[10] M. S. Grewal and L. Talbot, J. Fluid Mech. **16**, 573 [1963].
[11] M. Y. Jaffrin, Phys. Fluids **8**, 606 [1965].